

A Novel and Expanding SARS-CoV-2 Variant, B.1.526, Identified in New York

Medini K. Annavajhala^{1*}, Hiroshi Mohri^{2*}, Pengfei Wang², Manoj Nair², Jason E. Zucker¹, Zizhang Sheng², Angela Gomez-Simmonds¹, Anne L. Kelley¹, Maya Tagliavia¹, Yaoxing Huang², Trevor Bedford³, David D. Ho^{1,2,4#}, Anne-Catrin Uhlemann^{1#}

¹ Division of Infectious Diseases, Department of Internal Medicine, Columbia University Vagelos College of Physicians and Surgeons, New York, NY, USA

² Aaron Diamond AIDS Research Center, Columbia University Vagelos College of Physicians and Surgeons, New York, NY, USA

³ Vaccine and Infectious Disease Division, Fred Hutchinson Cancer Research Center, Seattle, WA, USA

⁴ Department of Microbiology and Immunology, Columbia University Irving Medical Center, New York, NY, USA.

* Medini K. Annavajhala and Hiroshi Mohri contributed equally to this work.

David D. Ho and Anne-Catrin Uhlemann contributed equally to this work.

Address correspondence to au2110@cumc.columbia.edu or dh2994@cumc.columbia.edu.

1 **Summary**

2 **Recent months have seen surges of SARS-CoV-2 infection across the globe along with**
3 **considerable viral evolution¹⁻³. Extensive mutations in the spike protein may threaten**
4 **efficacy of vaccines and therapeutic monoclonal antibodies⁴. Two signature mutations of**
5 **concern are E484K, which plays a crucial role in the loss of neutralizing activity of**
6 **antibodies, and N501Y, a driver of rapid worldwide transmission of the B.1.1.7 lineage. Here,**
7 **we report the emergence of a novel variant lineage B.1.526 that contains E484K and its**
8 **alarming rise to dominance in New York City in recent months. This variant is partially or**
9 **completely resistant to two therapeutic monoclonal antibodies in clinical use. It is also less**
10 **susceptible to neutralization by convalescent plasma or vaccinee sera, posing a modest**
11 **antigenic challenge. The B.1.526 lineage has now been reported from all 50 states in the US**
12 **and numerous other countries. B.1.526 has rapidly replaced non-variant lineages in New**
13 **York, with an estimated transmission advantage of 35%. Although B.1.526 initially outpaced**
14 **B.1.1.7 in the region, its growth has slowed concurrent with the rise of B.1.1.7. In states**
15 **surrounding New York, B.1.526 continues to increase where B.1.1.7 has not yet reached**
16 **dominance, persistently replacing non-variant lineages. Such transmission dynamics,**
17 **together with the relative antibody resistance of its E484K sub-lineage, would warrant**
18 **consideration of B.1.526 as a SARS-CoV-2 variant of concern.**

19
20

21 **Main**

22 While evolution of SARS-CoV-2 was deemed to be slow at the beginning of the global pandemic⁵,
23 at least four major variants of concern have emerged over the past six months^{1-3,6}. These lineages
24 are each characterized by numerous mutations in the spike protein, raising concerns that they may
25 escape from therapeutic monoclonals and vaccine-induced antibodies. The hallmark mutation of
26 B.1.1.7, a SARS-CoV-2 variant of concern that emerged in the UK, is N501Y located in the
27 receptor-binding domain (RBD) of spike¹. This variant is seemingly more transmissible and
28 virulent⁷⁻⁹, perhaps due to a higher binding affinity of N501Y for ACE2¹⁰ or a greater propensity
29 to evade host innate immune responses¹¹. Two other variants of concern, B.1.351 (first detected in
30 South Africa)² and P.1 (first described in travelers from Brazil to Japan)^{12,13}, share the N501Y
31 mutation with B.1.1.7 but also contain an E484K substitution in RBD^{2,3}. Epidemiological evidence
32 suggests that P.1 emerged as part of a second surge in Manaus, Brazil despite a high pre-existing
33 SARS-CoV-2 seroprevalence in the population¹⁴. Reinfections with P.1, as well as with another
34 related Brazilian variant P.2 that also harbors E484K, have been documented^{15,16}. Another variant
35 of concern is the B.1.617.2 lineage that recently emerged from India⁶.

36
37 Our previous study on B.1.351 demonstrated that this variant is refractory to neutralization by a
38 number of monoclonal antibodies directed to the top of RBD, including several that have received
39 emergency use authorization⁴. Moreover, this variant was markedly more resistant to
40 neutralization by convalescent plasma and vaccinee sera. Importantly, these effects were in part
41 mediated by the E484K mutation. These findings are worrisome in light of recent reports that three
42 vaccine trials showed a substantial drop in efficacy in South Africa¹⁷⁻¹⁹. Likewise, P.1 was also
43 relatively resistant to antibody neutralization, although not as severely²⁰. To systematically screen
44 our patient population in Northern Manhattan for B.1.351 and other E484K variants, as well as
45 B.1.1.7, we implemented a rapid PCR-based screen for signature mutations combined with
46 genomic surveillance.

47
48 **Rapid screening for signature SARS-CoV-2 mutations**
49 We first developed rapid PCR-based single-nucleotide-polymorphism assays to search for N501Y
50 and E484K mutations (see schematic in Extended Data Fig. 1) in clinical samples known to be
51 positive for SARS-CoV-2 and stored in the Columbia University Biobank, a biorepository of

52 SARS-CoV-2 patient specimens from hospitals and outpatient clinics within our medical system.
53 Patient and clinical testing information was extracted from the COVID-Care database²¹. Between
54 November 1, 2020 and May 1, 2021, 3,433 SARS-CoV-2-positive nasopharyngeal swabs were
55 available through the Columbia University Biobank for our study (Extended Data Fig. 2). We first
56 screened 2,174 samples collected between November 1, 2020 and March 5, 2020 for the two
57 signature mutations E484K and N501Y. There were 741 samples which were non-typeable and
58 showed no signal in either genotyping assay. We identified 155 samples with E484K (10.8% of
59 1,433 typeable samples) and 41/1,433 (2.9%) with N501Y. Only one sample contained both
60 mutations. The earliest case with E484K was collected in mid-November 2020. Subsequently,
61 there was a substantial increase in the proportion of E484K among PCR-screened cases over time
62 (Fig. 1a), from 2.0% at the end of 2020 to 24.3% between February 21st and March 5th, 2021, the
63 final two weeks of targeted PCR genotyping. Viruses harboring N501Y also increased over time,
64 from the earliest detection in mid-January to 5.3% of screened isolates by the beginning of March.
65

66 **Genomic surveillance of SARS-CoV-2**

67 We next performed untargeted whole genome nanopore sequencing of nasopharyngeal samples
68 collected throughout the study period with Ct \leq 35. We successfully obtained 1,210 SARS-CoV-2
69 whole genomes. This represents 70.4% of all samples with Ct values of 30 or below and 14.0% of
70 samples with Ct values between 30 and 35 (Extended Data Fig. 2). Sequencing results verified the
71 E484K and N501Y substitutions in all samples identified by our screening PCR assays. Amongst
72 PCR-screened cases with N501Y, 21/30 (70.0%) of sequenced N501Y isolates were identified as
73 belonging to the B.1.1.7 lineage. One sample which harbored both N501Y and E484K based on
74 our screening assay was identified as B.1.351. However, quite unexpectedly, the large majority of
75 PCR-screened cases with E484K (n=85/112, 75.9%) fell within a single lineage, B.1.526,²²
76 recently labeled the Iota variant by the WHO²³.

77
78 Analysis of the entire collection of CUIMC genomic sequences (Fig. 1b) shows that over the past
79 few months, SARS-CoV-2 variants (including B.1.526, B.1.1.7, and more recently P.1) now
80 comprise two-thirds of all sequenced isolates, replacing the vast majority of non-variant lineages
81 (Fig. 1b). The proportion of cases caused by B.1.526, including the B.1.526-S477N and B.1.526-
82 L452R sub-lineages, rose rapidly from late 2020 through February 2021, and has remained at

83 approximately 40-50% of all sequenced cases from March to May 2021, despite a concurrent
84 increase in B.1.1.7. In fact, during the months of December and January when the prevalence of
85 B.1.1.7 was still negligible (Fig. 1b, marking under horizontal axis), the frequency of all viruses
86 in the B.1.526 lineage rose from <5% to 50% while the frequency of non-variant viruses declined
87 from >95% to 50% (Fig. 1b, where white blank space represents non-variant viruses). Calculations
88 using these numbers in a head-to-head comparison and an established mathematical method²⁴
89 indicate that B.1.526 has a growth advantage of ~5% per day. Likewise, fitting a logistic regression
90 model to 478 individual observations from the extended timeframe of November 2020 through
91 January 2021 shows that B.1.526 has a similar growth advantage of 4.6% per day (95% CI 2.8–
92 6.5% per day). Given that the serial interval for SARS-CoV-2 transmission is about 7 days²⁵ in the
93 absence of any intervention, these results suggest that B.1.526 is ~35% more transmissible than
94 non-variant viruses. This is certainly a cause for concern.

95

96 **Signature mutations of the B.1.526 lineage**

97 We identified signature spike-protein mutations in the B.1.526 lineage by comparing all genomes
98 generated as a part of this study. In Figure 1c, all unique patterns of S-gene mutations in our
99 collection are displayed. Phylogenetic examination showed that the B.1.526 lineage is comprised
100 of two closely related sub-lineages harboring either E484K (B.1.526-E484K; defined as Pangolin
101 lineage B.1.526) or S477N (B.1.526-S477N; Pangolin lineage B.1.526.2) (Fig. 1c). In addition,
102 the sub-lineage B.1.526.1, which harbors the L452R substitution, has been more recently defined
103 (referred to in this study as B.1.526-L452R). Both B.1.526-E484K and B.1.526-S477N share
104 characteristic spike-protein mutations L5F, T95I, D253G, D614G, and either A701V or Q957R
105 along with either E484K or S477N. Non-spike mutations widely shared by B.1.526-E484K and
106 B.1.526-S477N isolates include: T85I in ORF1a-nsp2; L438P in ORF1a-nsp4, a 9bp deletion
107 Δ 106-108 in ORF1a-nsp6; P323L in ORF1b-nsp12; Q88H in ORF1b-nsp13; Q57H in ORF3a; and
108 P199L and M234I in the N gene. While B.1.526-L452R isolates shared a number of mutations
109 across the genome in ORF-1ab, ORF-3ab, ORF-8, and N, it does not share spike mutations with
110 B.1.526-E484K and B.1.526-S477N except for D614G, which is ubiquitous in presently
111 circulating SARS-CoV-2 lineages.

112

113 To further investigate the evolutionary history of B.1.526, we performed phylogenetic analyses on
114 genomes in this collection and in GISAID harboring the 9bp deletion Δ 106-108 in ORF1a-nsp6,
115 along with mutation A20262G that uniquely defines the parent clade containing B.1.526 and
116 related viruses (Fig. 2a). We observed a stepwise emergence of the key lineage-defining mutations,
117 with T95I, D253G, and L5F appearing in the earliest phylogenetic nodes. Isolates subsequently
118 branched into four sub-lineages, with two major groups B.1.526-E484K and B.1.526-S477N
119 containing A701V, with a smaller sub-lineage B.1.526-S477N containing Q957R. The B.1.526-
120 L452R lineage also emerged in parallel, as a distinct branch from other B.1.526 lineages.

121
122 Fig. 2b displays the localization of B.1.526-E484K and B.1.526-S477N signature spike mutations
123 within the S protein. D253G resides in the antigenic supersite within the N-terminal domain²⁶,
124 which is a target for neutralizing antibodies²⁷, whereas the E484K is situated at the RBD interface
125 with the cellular receptor ACE2. The A701V mutation near the furin cleavage site is also shared
126 with variant B.1.351.

127 128 **Antibody neutralization of B.1.526**

129 The impact of the signature S protein mutations in B.1.526 on antibody neutralization was first
130 assessed using vesicular stomatitis virus (VSV) based pseudoviruses as previously described^{4,27}.
131 Pseudoviruses containing S477N or E484K alone and all five signature mutations (L5F, T95I,
132 D253G, A701V, and E484K or S477N), termed NY Δ 5(E484K) or NY Δ 5(S477N), were
133 constructed and subjected to neutralization by 12 monoclonal antibodies including 5 with
134 emergency use authorization, 20 convalescent plasma, and 22 vaccinee sera. The specifics of these
135 monoclonal antibodies and clinical specimens were previously reported⁴. As shown in Extended
136 Data Fig. 3a, the neutralizing activity of 12 monoclonal antibodies covering a range of epitopes on
137 RBD was essentially unaltered against the S477N and NY Δ 5(S477N) pseudoviruses, showing that
138 this mutation has no discernible antigenic impact, as was confirmed using convalescent plasma
139 and vaccinee sera (Extended Data Fig. 3b). However, against E484K and NY Δ 5(E484K)
140 pseudoviruses, the activities of several antibodies were either impaired or lost, including
141 REGN10933 and LY-CoV555 that are already in clinical use (Fig. 3a). Likewise, neutralizing
142 activities of convalescent plasma or vaccinee sera were lowered by 4.1-fold or 3.3-3.6-fold,
143 respectively, against NY Δ 5(E484K) (Fig. 3b) but not against NY Δ 5(S477N) (Extended Data Fig.

144 3b). Neutralization studies of the authentic B.1.526-E484K virus yielded similar results, although
145 the magnitude of resistance to convalescent plasma or vaccinee sera was slightly lower at 2.6-fold
146 or 1.8-2.0-fold, respectively (Fig. 3b). A comparative analysis with other variants of concern (Fig.
147 3c) showed that such risks are likely lower than B.1.351 and closer to P.1. Overall, these results
148 demonstrate the need to modify our antibody therapy and to monitor the efficacy of current
149 vaccines in regions where B.1.526-E484K is prevalent.

150

151 **Clinical comparisons of patients infected with E484K and B.1.526 versus non-variant viral** 152 **strains**

153 Patients with E484K variant viruses were comparable in gender, age, race and ethnicity to those
154 with SARS-CoV-2 strains not harboring either E484K or N501Y (Extended Data Table 1). Patients
155 with E484K SARS-CoV-2 were more likely to live in New York City and Yonkers versus
156 elsewhere ($p=0.017$). E484K-positive patients had a higher rate of diabetes mellitus (32.2 vs
157 24.1%, $p=0.045$). The highest level of care required and the need for oxygen supplementation were
158 comparable between groups. Notably, the cycle threshold (Ct) values for E484K isolates were
159 significantly lower than isolates not harboring E484K (mean 29.49 vs 30.71, $p=0.013$), indicating
160 a modestly higher viral load in these variant samples. Comparison of cases of B.1.526-E484K
161 versus those with non-variant lineages²⁸ similarly showed no significant differences in
162 demographic characteristics. B.1.526-E484K was also associated with a significantly higher
163 proportion of patients with diabetes mellitus (30.8 vs 21.7%, $p=0.014$) as well as higher BMI (28.4
164 versus 26.5 kg/m², $p=0.008$). We also found a lower cycle threshold value associated with B.1.526-
165 E484K (27.33 vs 28.31 in non-variant lineages, $p=0.041$). Notably, a significantly higher
166 proportion of patients B.1.526-E484K were admitted to the hospital or presented to the emergency
167 department, and a lower proportion received only outpatient care ($p=0.041$).

168

169 **Surge of B.1.526 across New York and the U.S.**

170 Prevalence of the novel variant B.1.526 has surged alarmingly in our hospital catchment area (Fig.
171 4a) and throughout New York State (Fig. 4b) since its emergence in late 2020, replacing non-
172 variant lineages and initially outpacing B.1.1.7. A multinomial logistic regression model
173 describing the concurrent growth rates of these two lineages shows that starting in mid-April 2021,
174 B.1.1.7 surpassed B.1.526 due to a slightly higher fitness, with estimated growth rates in New

175 York State of 5.3% per day for B.1.1.7 (95% CI 5.0–5.7%) and 3.4% per day for B.1.526 (3.2–
176 3.6%) (Fig. 4b). These estimates suggest a fitness advantage of B.1.526 over existing non-variant
177 lineages of 22–25% over a serial interval of 7 days^{24,25} during a period when multiple variants are
178 competing simultaneously. Furthermore, the estimates also suggest a fitness advantage of B.1.1.7
179 over existing non-variant lineages of 35–40%, as well as a fitness advantage of B.1.1.7 over
180 B.1.526 of 12–15%. As shown in Figs. 4a and 4b, both lineages grew quickly, but once they
181 reached a high frequency of circulating viruses, the competition between them caused the growth
182 of B.1.1.7 to slow and B.1.526 to decline.

183
184 Frequency trajectories of B.1.1.7 and B.1.526 across states (Fig. 4c, Extended Data Fig. 4) show
185 two general patterns: (1) initial rapid increase of both lineages until the proportion of other lineages
186 had been eclipsed, followed by decline of B.1.526 seen in New York and in several neighboring
187 states; and (2) rapid growth and resulting dominance of B.1.1.7 preventing the further rise of
188 B.1.526. The dynamics between these two lineages is further shown in Fig. 4d, which plots the
189 logistic growth rate of B.1.526 against the frequency of B.1.1.7, again at the state-level. At lower
190 frequencies of B.1.1.7, all states have a similarly rapid growth of B.1.526 as it replaces non-variant
191 lineages. As B.1.1.7 increases in frequency, however, it slows the growth of B.1.526, again
192 indicative of a slightly higher fitness for B.1.1.7. At a minimum, B.1.526 is rising rapidly where
193 B.1.1.7 is not dominant and, in several states, has continued to grow at a similar pace as B.1.1.7
194 (Extended Data Fig. 4).

195
196 Phylogeographic analysis of viruses designated as belonging to the B.1.526 lineage shows
197 ancestral viruses originating in New York in August 2020, diversifying within the state, and then
198 dispersing to other states (Figs. 4e and 4f). State-level genomic data show that B.1.526 is
199 concentrated primarily in New York and surrounding states, including New Jersey and Rhode
200 Island (Extended Data Fig. 4). This suggests that B.1.526, and B.1.526-E484K in particular, is
201 now widespread in the region, the original epicenter of COVID-19 in the US^{29,30}, although the
202 lineage has also grown in states outside the Northeastern US (e.g., North Carolina). By the end of
203 April 2021, the geographic makeup of B.1.526 within the US has become quite diverse, and the
204 lineage has emerged and expanded in multiple states across the country (Fig. 4f). Of particular

205 concern is the rise of B.1.526 over the past six months across the United States (Extended Data
206 Fig. 4), as well as its international spread.

207

208 **Discussion**

209 Here we report the emergence of a novel SARS-CoV-2 lineage, B.1.526, and its alarming surge in
210 New York during the second wave of the COVID-19 pandemic (Fig. 1b). Neutralization studies
211 on B.1.526-E484K demonstrate that the activities of several antibodies were either impaired or
212 lost, including two (Ly-CoV555 and REGN10933) already in clinical use (Fig. 3a). Furthermore,
213 neutralizing activities of convalescent plasma or vaccinee sera were lower against B.1.526
214 harboring E484K (Fig. 3b). These findings are of concern, and it will be important to monitor the
215 antigenic impact of this variant on re-infection or vaccine breakthrough in the future. The S477N
216 mutation, a key signature of another B.1.526 sub-lineage, on the other hand, did not have an impact
217 on antibody neutralizing (Extended Data Fig. 3).

218

219 Several limitations of our study need to be considered. This was a single-center genomic survey
220 representing patients presenting to a hospital system and may not have fully captured patients with
221 milder disease. However, we note that our results are comparable to genomic data released by
222 public health laboratories in the region and further incorporate all publicly available data for
223 phylogeographic context and growth rate calculations. As in all genomic surveillance studies, we
224 predominantly sequenced samples with a Ct of < 30 but covered a high proportion of samples
225 throughout the study period. In addition, our PCR screen allowed us to obtain unbiased estimates
226 of E484K and N501Y prevalence early on in the study. PCR approaches may be increasingly
227 warranted now for continued surveillance, as new infection rates are lower in the US and Ct values
228 are higher during non-surge periods. Lastly, transmissibility estimates based on observed
229 prevalence are imperfect as they reflect observed growth rates rather than intrinsic transmissibility
230 of the virus.

231

232 Taken together, our findings underscore the importance of the E484K mutation, which has
233 emerged in at least 246 different lineages of SARS-CoV-2³¹, a real testament to convergent
234 evolution. This raises the possibility that E484K can rapidly emerge in multiple clonal
235 backgrounds and may warrant targeted screening for this key mutation in addition to robust

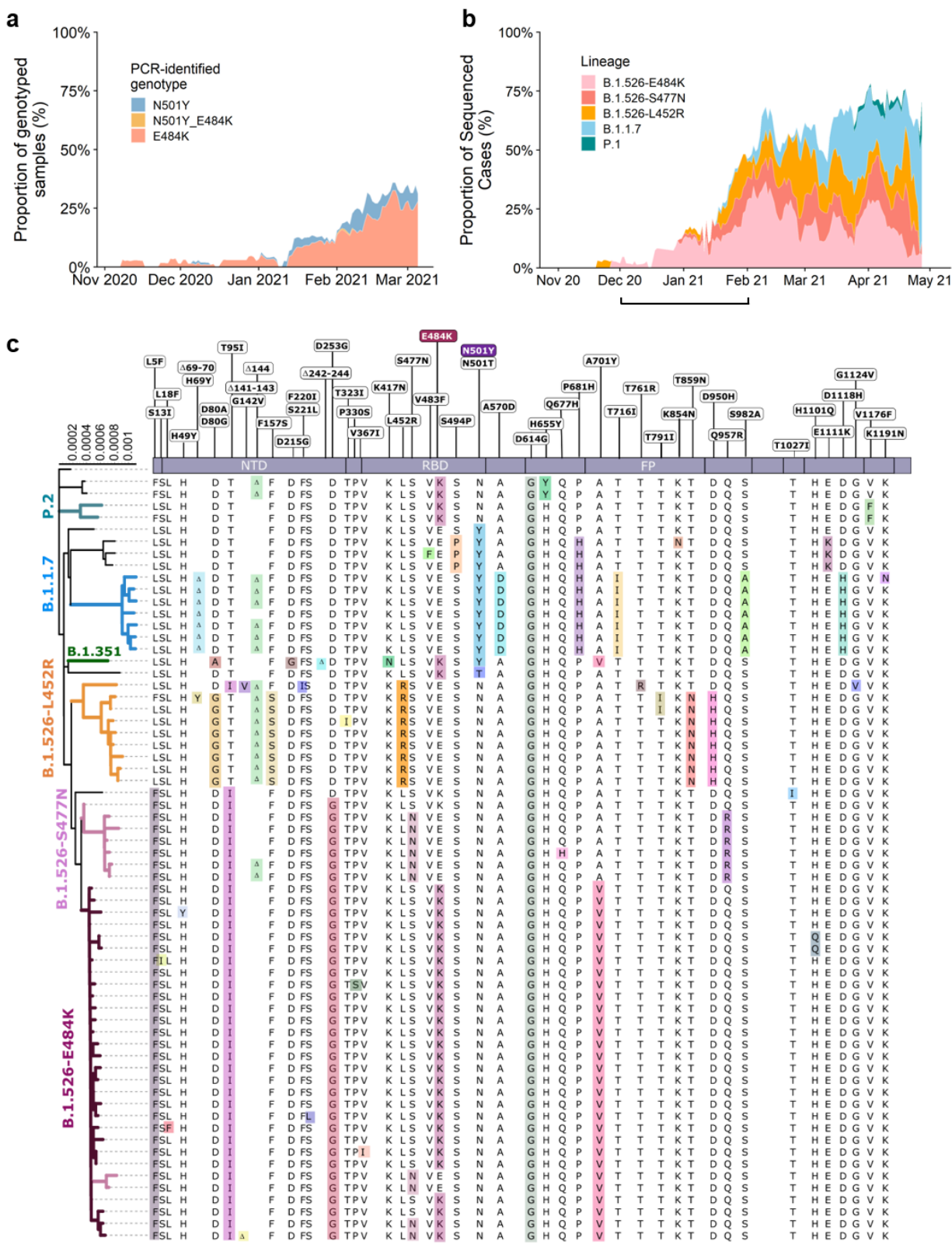
236 genomic surveillance programs. However, B.1.526 is one of the few lineages with E484K that has
237 risen to prominence. The greatest threat of B.1.526 appears to be its ease of spread, with an
238 estimated transmissibility of ~35% greater than non-variant viruses when competing head-to-head.
239 Despite the higher observed fitness of B.1.1.7, B.1.526 was able to spread rapidly in the US to
240 replace other lineages and has continued to increase in frequency in several states. This apparent
241 increased transmissibility is of particular concern, especially given the relative antibody resistance
242 of the sub-lineage with the E484K mutation (Fig. 3c). While B.1.1.7 may be the most transmissible
243 variant identified to date and B.1.351 may pose the greatest antigenic challenge to antibodies and
244 vaccines, B.1.526 is concerning because it has worrisome features of both. Overall, the
245 identification of B.1.526 reported here serves to highlight the need for concerted local, national,
246 and international surveillance programs to track and contain the spread of novel SARS-CoV-2
247 variants.

248 References

- 249 1 Rambaut, A. *et al.* Preliminary genomic characterisation of an emergent SARSCoV-2
250 lineage in the UK defined by a novel set of spike mutations. ,
251 <[https://virological.org/t/preliminary-genomic-characterisation-of-an-emergent-
252 sars-cov-2-lineage-in-the-uk-defined-by-a-novel-set-of-spike-mutations/563](https://virological.org/t/preliminary-genomic-characterisation-of-an-emergent-sars-cov-2-lineage-in-the-uk-defined-by-a-novel-set-of-spike-mutations/563)>
253 (2020).
- 254 2 Tegally, H. *et al.* Emergence and rapid spread of a new severe acute respiratory
255 syndrome-related coronavirus 2 (SARS-CoV-2) lineage with multiple spike mutations
256 in South Africa. *medRxiv*, 2020.2012.2021.20248640,
257 doi:10.1101/2020.12.21.20248640 (2020).
- 258 3 Faria, N. R. *et al.* Genomic characterisation of an emergent SARS-CoV-2 lineage in
259 Manaus: preliminary findings. (2021).
- 260 4 Wang, P. *et al.* Antibody Resistance of SARS-CoV-2 Variants B.1.351 and B.1.1.7.
261 *Nature*, doi:10.1038/s41586-021-03398-2 (2021).
- 262 5 Duchene, S. *et al.* Temporal signal and the phylodynamic threshold of SARS-CoV-2.
263 *Virus Evol* **6**, veaa061, doi:10.1093/ve/veaa061 (2020).
- 264 6 Cherian, S. *et al.* Convergent evolution of SARS-CoV-2 spike mutations, L452R, E484Q
265 and P681R, in the second wave of COVID-19 in Maharashtra, India. *bioRxiv*,
266 2021.2004.2022.440932, doi:10.1101/2021.04.22.440932 (2021).
- 267 7 Iacobucci, G. Covid-19: New UK variant may be linked to increased death rate, early
268 data indicate. *BMJ* **372**, n230, doi:10.1136/bmj.n230 (2021).
- 269 8 Volz, E. *et al.* Transmission of SARS-CoV-2 Lineage B.1.1.7 in England: Insights from
270 linking epidemiological and genetic data. *medRxiv*, 2020.2012.2030.20249034,
271 doi:10.1101/2020.12.30.20249034 (2021).
- 272 9 Washington, N. L. *et al.* Genomic epidemiology identifies emergence and rapid
273 transmission of SARS-CoV-2 B.1.1.7 in the United States. *medRxiv*,
274 doi:10.1101/2021.02.06.21251159 (2021).
- 275 10 Greaney, A. J. *et al.* Comprehensive mapping of mutations in the SARS-CoV-2 receptor-
276 binding domain that affect recognition by polyclonal human plasma antibodies. *Cell*
277 *Host Microbe* **29**, 463-476 e466, doi:10.1016/j.chom.2021.02.003 (2021).
- 278 11 Thorne, L. G. *et al.* Evolution of enhanced innate immune evasion by the SARS-CoV-2
279 B.1.1.7 UK variant. *bioRxiv*, 2021.2006.2006.446826,
280 doi:10.1101/2021.06.06.446826 (2021).
- 281 12 Fujino, T. *et al.* Novel SARS-CoV-2 Variant in Travelers from Brazil to Japan. *Emerg*
282 *Infect Dis* **27**, doi:10.3201/eid2704.210138 (2021).
- 283 13 Faria, N. R. *et al.* Genomics and epidemiology of the P.1 SARS-CoV-2 lineage in Manaus,
284 Brazil. *Science*, doi:10.1126/science.abh2644 (2021).
- 285 14 Sabino, E. C. *et al.* Resurgence of COVID-19 in Manaus, Brazil, despite high
286 seroprevalence. *Lancet* **397**, 452-455, doi:10.1016/S0140-6736(21)00183-5 (2021).
- 287 15 Zucman, N., Uhel, F., Descamps, D., Roux, D. & Ricard, J. D. Severe reinfection with
288 South African SARS-CoV-2 variant 501Y.V2: A case report. *Clin Infect Dis*,
289 doi:10.1093/cid/ciab129 (2021).
- 290 16 Nonaka, C. K. V. *et al.* Genomic Evidence of SARS-CoV-2 Reinfection Involving E484K
291 Spike Mutation, Brazil. *Emerg Infect Dis* **27**, doi:10.3201/eid2705.210191 (2021).

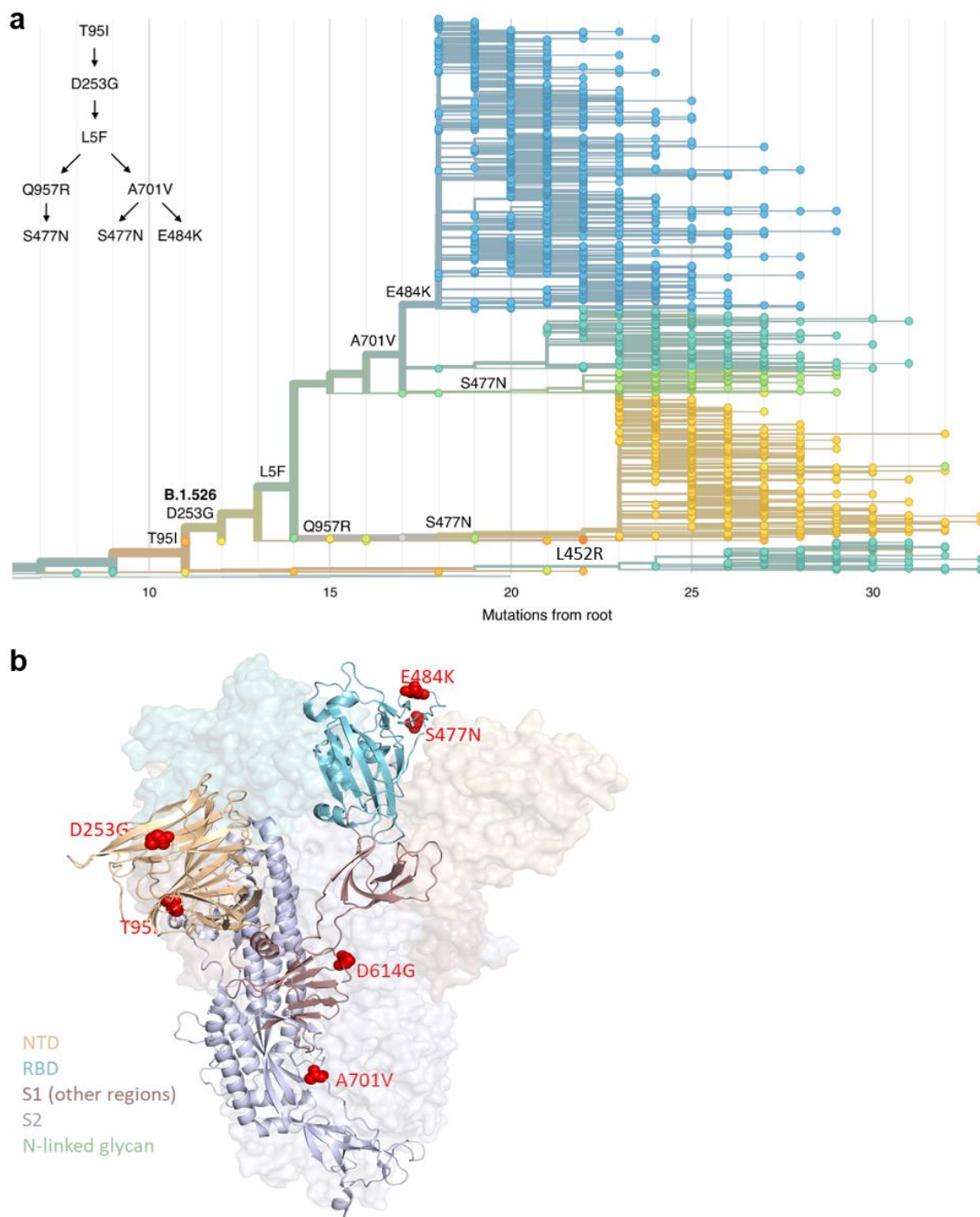
- 292 17 Wadman, M. & Cohen, J. *Novavax vaccine delivers 89% efficacy against COVID-19 in*
293 *U.K.—but is less potent in South Africa*,
294 <<https://www.sciencemag.org/news/2021/01/novavax-vaccine-delivers-89->
295 [efficacy348against-covid-19-uk-less-potent-south-africa](https://www.sciencemag.org/news/2021/01/novavax-vaccine-delivers-89-)> (2021).
- 296 18 Callaway, E. & Mallapaty, S. Novavax offers first evidence that COVID vaccines protect
297 people against variants. *Nature* **590**, 17, doi:10.1038/d41586-021-00268-9 (2021).
- 298 19 Madhi, S. A. *et al.* Efficacy of the ChAdOx1 nCoV-19 Covid-19 Vaccine against the
299 B.1.351 Variant. *N Engl J Med*, doi:10.1056/NEJMoa2102214 (2021).
- 300 20 Wang, P. *et al.* Increased Resistance of SARS-CoV-2 Variant P.1 to Antibody
301 Neutralization. *bioRxiv*, doi:10.1101/2021.03.01.433466 (2021).
- 302 21 Miller, E. H. *et al.* Pretest Symptom Duration and Cycle Threshold Values for Severe
303 Acute Respiratory Syndrome Coronavirus 2 Reverse-Transcription Polymerase Chain
304 Reaction Predict Coronavirus Disease 2019 Mortality. *Open Forum Infectious Diseases*
305 **8**, doi:10.1093/ofid/ofab003 (2021).
- 306 22 West, A. P., Barnes, C. O., Yang, Z. & Bjorkman, P. J. SARS-CoV-2 lineage B.1.526
307 emerging in the New York region detected by software utility created to query the
308 spike mutational landscape. *bioRxiv*, 2021.2002.2014.431043,
309 doi:10.1101/2021.02.14.431043 (2021).
- 310 23 WHO. *Tracking SARS-CoV-2 Variants*, <[https://www.who.int/en/activities/tracking-](https://www.who.int/en/activities/tracking-SARS-CoV-2-variants/)
311 [SARS-CoV-2-variants/](https://www.who.int/en/activities/tracking-SARS-CoV-2-variants/)> (2021).
- 312 24 Goudsmit, J., De Ronde, A., Ho, D. D. & Perelson, A. S. Human immunodeficiency virus
313 fitness in vivo: calculations based on a single zidovudine resistance mutation at codon
314 215 of reverse transcriptase. *J Virol* **70**, 5662-5664, doi:10.1128/JVI.70.8.5662-
315 5664.1996 (1996).
- 316 25 Ali, S. T. *et al.* Serial interval of SARS-CoV-2 was shortened over time by
317 nonpharmaceutical interventions. *Science* **369**, 1106-1109,
318 doi:10.1126/science.abc9004 (2020).
- 319 26 Cerutti, G. *et al.* Potent SARS-CoV-2 Neutralizing Antibodies Directed Against Spike N-
320 Terminal Domain Target a Single Supersite. *bioRxiv*, 2021.2001.2010.426120,
321 doi:10.1101/2021.01.10.426120 (2021).
- 322 27 Liu, L. *et al.* Potent neutralizing antibodies against multiple epitopes on SARS-CoV-2
323 spike. *Nature* **584**, 450-456, doi:10.1038/s41586-020-2571-7 (2020).
- 324 28 CDC. *SARS-CoV-2 Variant Classifications and Definitions*, <SARS-CoV-2 Variant
325 Classifications and Definitions> (2021).
- 326 29 Health, N. Y. C. D. o. *COVID-19: Data*, <[https://www1.nyc.gov/site/doh/covid/covid-](https://www1.nyc.gov/site/doh/covid/covid-19-data-trends.page#antibody)
327 [19-data-trends.page#antibody](https://www1.nyc.gov/site/doh/covid/covid-19-data-trends.page#antibody)> (2021).
- 328 30 Lasek-Nesselquist, E., Lapierre, P., Schneider, E., George, K. S. & Pata, J. The localized
329 rise of a B.1.526 SARS-CoV-2 variant containing an E484K mutation in New York
330 State. *medRxiv*, 2021.2002.2026.21251868, doi:10.1101/2021.02.26.21251868
331 (2021).
- 332 31 Alaa Abdel Latif, K. G., Julia L. Mullen, Emily Haag, Ginger Tsueng, Nate Matteson, Mark
333 Zeller, Chunlei Wu, Kristian G. Andersen, Andrew I. Su, Laura D. Hughes, and the
334 Center for Viral Systems. *B.1.526 Lineage Report*, <[https://outbreak.info/situation-](https://outbreak.info/situation-reports/S-E484K)
335 [reports/S-E484K](https://outbreak.info/situation-reports/S-E484K)> (2021).

- 336 32 Smyrlaki, I. *et al.* Massive and rapid COVID-19 testing is feasible by extraction-free
337 SARS-CoV-2 RT-PCR. *Nat Commun* **11**, 4812, doi:10.1038/s41467-020-18611-5
338 (2020).
- 339 33 Quick, J. *Artic Protocol*, <[https://www.protocols.io/view/ncov-2019-sequencing-
340 protocol-v3-locost-bh42j8ye](https://www.protocols.io/view/ncov-2019-sequencing-protocol-v3-locost-bh42j8ye)> (2021).
- 341 34 Freed, N., Vlkova, M., Faisal, M. B. & Silander, O. Rapid and inexpensive whole-genome
342 sequencing of SARS-CoV2 using 1200 bp tiled amplicons and Oxford Nanopore rapid
343 barcoding. *bioRxiv*, doi:10.1101/2020.05.28.122648 (2020).
- 344 35 Hadfield, J. *et al.* Nextstrain: real-time tracking of pathogen evolution. *Bioinformatics*
345 **34**, 4121-4123, doi:10.1093/bioinformatics/bty407 (2018).
- 346 36 Minh, B. Q. *et al.* IQ-TREE 2: New Models and Efficient Methods for Phylogenetic
347 Inference in the Genomic Era. *Mol Biol Evol* **37**, 1530-1534,
348 doi:10.1093/molbev/msaa015 (2020).
- 349 37 Sagulenko, P., Puller, V. & Neher, R. A. TreeTime: Maximum-likelihood phylodynamic
350 analysis. *Virus Evol* **4**, vex042, doi:10.1093/ve/vex042 (2018).
- 351 38 Shu, Y. & McCauley, J. GISAID: Global initiative on sharing all influenza data - from
352 vision to reality. *Euro Surveill* **22**, doi:10.2807/1560-7917.ES.2017.22.13.30494
353 (2017).
- 354 39 Pinto, D. *et al.* Cross-neutralization of SARS-CoV-2 by a human monoclonal SARS-CoV
355 antibody. *Nature* **583**, 290-295, doi:10.1038/s41586-020-2349-y (2020).
- 356 40 Zost, S. J. *et al.* Rapid isolation and profiling of a diverse panel of human monoclonal
357 antibodies targeting the SARS-CoV-2 spike protein. *Nat Med* **26**, 1422-1427,
358 doi:10.1038/s41591-020-0998-x (2020).
- 359 41 Robbiani, D. F. *et al.* Convergent antibody responses to SARS-CoV-2 in convalescent
360 individuals. *Nature* **584**, 437-442, doi:10.1038/s41586-020-2456-9 (2020).
- 361 42 Rambaut, A. *et al.* A dynamic nomenclature proposal for SARS-CoV-2 lineages to assist
362 genomic epidemiology. *Nat Microbiol* **5**, 1403-1407, doi:10.1038/s41564-020-0770-
363 5 (2020).
- 364
- 365



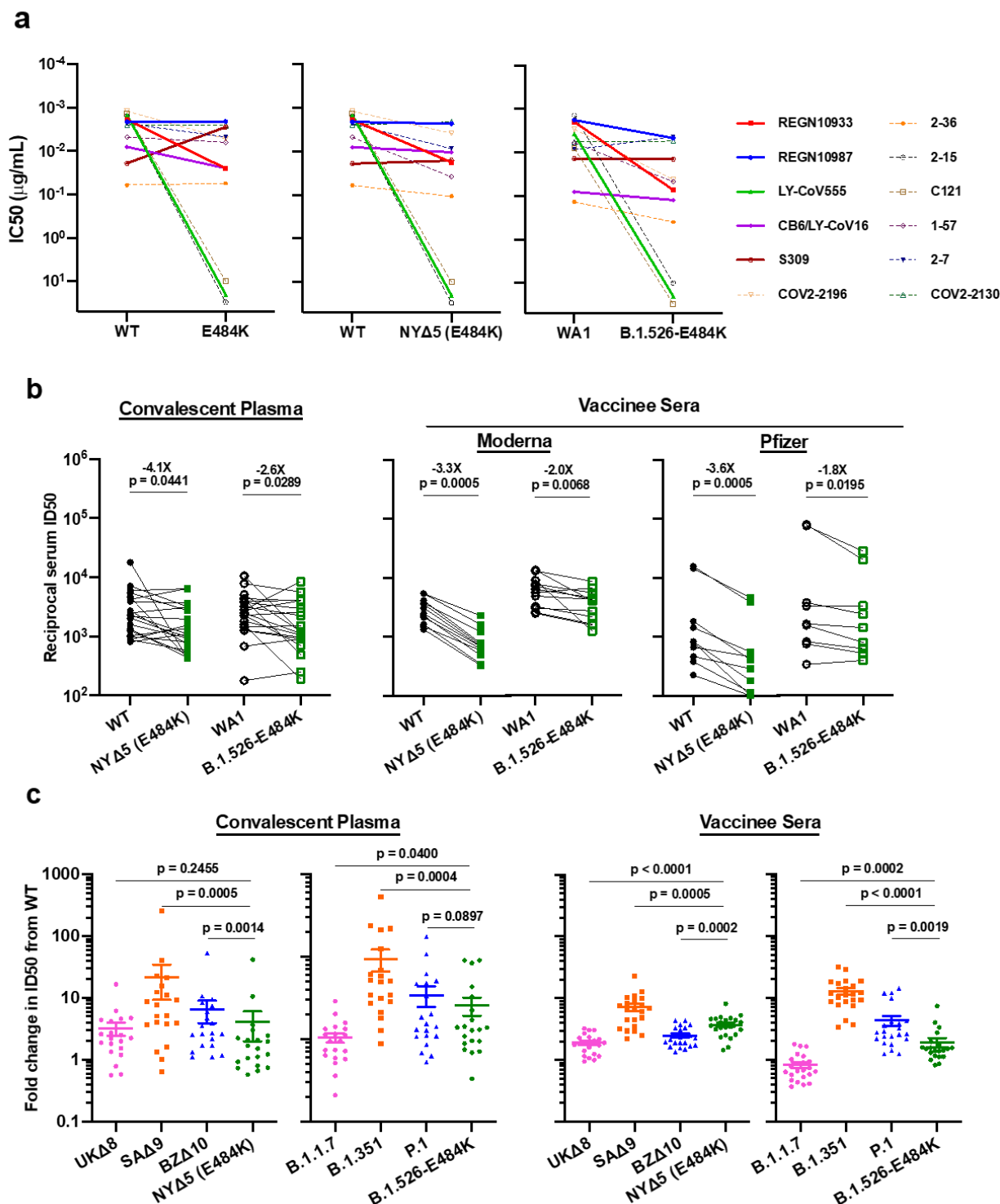
366

367 **Figure 1. Prevalence of E484K-harboring SARS-CoV-2 and B.1.526.** (a) Detection of viruses
368 with key signature mutations in spike over time. The earliest detected E484K-harboring variant
369 was collected in mid-November 2020. The prevalence of E484K ($n_{E484K}/(n_{\text{screened}} + n_{E484K})$)
370 subsequently increased over time, from 4.8% in early December 2020 up to 24.3% in early March
371 2021. Throughout late 2020 and early 2021, we identified fewer N501Y- than E484K-harboring
372 isolates, with a maximum of 5.9% of N501Y during mid-February 2021. (b) Distribution of
373 different viral lineages identified by whole genome sequencing. Within our genomic collection
374 ($n=1,210$), the B.1.526 lineage rose rapidly in early 2021, replacing the majority of non-variant
375 lineages (shown as the white blank space) present during this timeframe. This was followed by a
376 steady rise in B.1.1.7 by mid-2021. The marking below the X axis denotes the time period used to
377 calculate the growth advantage of B.1.526 over non-variant viruses. (c) Phylogenetic tree of
378 SARS-CoV-2 variants identified by sequencing and alignment of key spike mutations. Unique
379 patterns of spike protein mutations present in genomes sequenced from our hospital center with at
380 least one mutation of interest or concern (E484K, N501Y, S477N, or L452R; $n=64$) are shown.
381 Residues at which at least one sample harbored a mutation are displayed above the S-protein
382 schematic.
383
384



385
386 **Figure 2. Spike protein amino acid substitutions and structural changes represented in**
387 **sequenced isolates.** Three amino acid changes are characteristic of the B.1.526 lineage: L5F, T95I,
388 D253G with sub-lineages possessing additional changes S477N, E484K, A701V and Q957R. (a)
389 Maximum-likelihood phylogenetic tree of 2309 SARS-CoV-2 viruses colored according to spike
390 protein haplotype. Spike protein mutations are labeled on the tree showing the stepwise

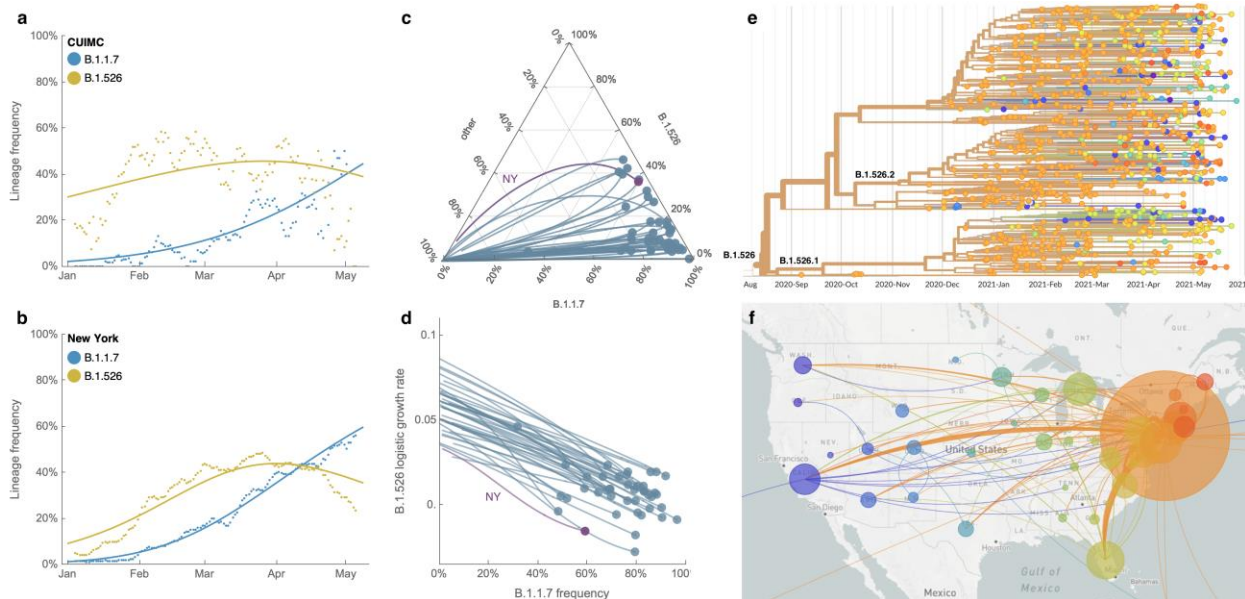
391 accumulation of signature B.1.526 mutations and branching of the B.1.526-E484K and B.1.526-
392 S477N sub-lineages. An interactive version of this figure is available at
393 <https://nextstrain.org/groups/blab/ncov/ny/B.1.526>. **(b)** Key mutations of B.1.526 displayed on the
394 spike trimer. The D253G mutation resides in the antigenic supersite within the N-terminal domain
395 (NTD), a target for neutralizing antibodies, E484K and S477N at the receptor binding domain
396 (RBD) interface with the cellular receptor ACE2, and A701V near the furin cleavage site.



397
 398 **Figure 3. Neutralization studies of B.1.526-E484K and comparative analyses.** (a) Neutralizing
 399 activities of 12 monoclonal antibodies against pseudoviruses containing E484K alone or all five
 400 signature B.1.526 mutations (L5F, T95I, D253G, A701V, and E484K), termed NY Δ 5(E484K) as

401 well as against the authentic B.1.526-E484K. Antibodies with emergency use authorization are
402 shown in bold solid lines. **(b)** Neutralizing activities of convalescent plasma (n=20) and vaccinee
403 sera (n=22) against the NYΔ5(E484K) pseudovirus compared to wildtype pseudovirus as well as
404 against authentic B.1.526-E484K and wildtype virus (WA1). **(c)** Fold change in convalescent
405 plasma and vaccinee sera neutralization ID50 of different variant pseudoviruses and live viruses
406 compared to wildtype counterparts. The data on B.1.1.7, B.1.351 and P.1 were derived from our
407 prior publications^{4,20}. Data from 20 convalescent patients or 22 vaccinated individuals were
408 averaged and are represented as arithmetic mean \pm SEM.
409

410



411

412 **Figure 4. Spread of lineages B.1.1.7 and B.1.526 in New York and the USA.** (a, b) Frequencies
413 of lineages B.1.1.7 (blue) and B.1.526 (yellow) in the CUIMC catchment area (in panel a) and
414 New York State (in panel b) with dots representing daily 7-day sliding window averages and lines
415 representing fit to a multinomial logistic regression model. (c) Ternary plot of state-level frequency
416 trajectories for 42 states separating frequencies of B.1.1.7, B.1.526 and other lineages. Each state-
417 level trajectory is a line in this plot moving from lower left in January 2021 when both B.1.1.7 and
418 B.1.526 were rare, rightward as B.1.1.7 and B.1.526 increase in frequency. The trajectory of New
419 York State is highlighted in purple. (d) The same data as in panel c, except plotting frequency of
420 B.1.1.7 against logistic growth rate of B.1.526. (e) Phylogenetic tree of 933 B.1.526 samples from
421 across the US where branch tips are colored based on location of sampling and branches are
422 colored by inferred ancestral location. (f) Phylogeographic view of data from panel e, where each
423 sampling location is represented as a circle with area proportional to sample count and each
424 inferred transition event across the phylogeny is drawn as an arc connecting inferred origin and
425 destination. Most migration events are inferred to be direct dispersals from New York State.

426 **Methods**

427 **Clinical cohort.** This observational study took place at an academic quaternary care center in New
428 York City. Nasopharyngeal swabs obtained as part of routine clinical care were tested by the
429 Clinical Microbiology laboratory, and positive specimens were transferred to the Columbia
430 University Biobank for inactivation and storage. Electronic health records data extracted for this
431 analysis included demographics, laboratory results, admission, discharge, and transfer dates,
432 current and historical international classification of disease (ICD 9 and 10) codes extracted from
433 the clinical data warehouse. This study was reviewed and approved by the Columbia University
434 Institutional Review Board (protocol number AAAT0123).

435
436 **PCR screening.** Extended Data Figure 1 describes our overall protocol for variant screening. To
437 enable rapid PCR-based screening, we prepared RNA using the heat inactivation method in place
438 of RNA isolation methods³². First, 50 μ l of nasal swab sample in VTM solution was transferred
439 into 96-well PCR plates, covered with an adhesive aluminum foil (VWR 60941-076) and
440 incubated at 95°C for 5 min using the PCR instrument. After the centrifugation of the plate at
441 $>2,100 \times g$ for 5 min, 5 μ l of the supernatant from each sample, which contains viral RNA, was
442 used for the SNP assay.

443
444 The SNP assay consists of four steps as follows: reverse transcription (RT) of viral RNA, pre-read
445 of the SNP assay, real-time PCR and post-read of the SNP assay. 5 μ l of RNA from the supernatant
446 was added to 15 μ l of the single step RT-qPCR reaction mix, which consists of 5 μ l of TaqPath 1-
447 step RT-qPCR Master Mix, CG (4x) (ThermoFisher Scientific), 500 nM of forward and reverse
448 primers, 120 nM of VIC-MGB probe, 50 nM of FAM-MGB probe, 1/2000 volume of ROX
449 Reference Dye (Invitrogen) as the final concentration, and nuclease-free water to adjust the total
450 reaction volume of 20 μ l. Each reaction plate included 8 control wells, 5×10^6 and 5×10^3 copies of
451 WA-1 (wild type), UK variant and South African variant, which were generated by PCR to match
452 the variant sequences, and 2 wells with water as no template controls (NTC).

453
454 The primer pairs and probes used are as follows. For the SNP assay for position **501**, a primer
455 pair of 501.F: 5'-GGT TTT AAT TGT TAC TTT CCT TTA CA-3' and 501.R: 5'-AGT TCA
456 AAA GAA AGT ACT ACT ACT CTG TAT G-3' were used with two TaqMan probes

457 (ThermoFisher Scientific), one for wild type, VIC.N501MGB: [VIC]-AA CCC ACT AAT
458 GGT-MGBNFQ and the other for variant type, FAM.Y501MGB: [FAM]-AAC CCA CTT ATG
459 GT-MGBNFQ. For position **484**, a primer pair of 484.F: 5'-AGA GAG ATA TTT CAA CTG
460 AAA TCT ATCAGG-3' and 484.R: 5'-GAA ACC ATA TGA TTG TAA AGG AAA GTA AC-
461 3' were used with two probes, one for wild type, VIC.E484MGB: [VIC]-ATG GTG TTG AAG
462 GT-MGBNFQ and the other for variant type, FAM.K484MGB: [FAM]-ATG GTG TTA AAG
463 GT-MGBNFQ. For position **477**, the primer pair of 477.F and 477.R was used with two probes,
464 one for wild type, VIC.S477MGB: [VIC]-TTA CAA GGT GTG CTA CCG-MGBNFQ and the
465 other for variant type, FAM.N477MGB: [FAM]-TTA CAA GGT GTG TTA CCG-MGBNFQ.
466

467 The reaction plate was subjected to 1) reverse-transcription reaction (RT) at the condition at 25°C
468 for 2 min, at 50°C for 15 min and a hold at 4°C; 2) SNP assay (pre-read) at 60°C for 30 sec; 3)
469 real-time PCR at 95°C for 20 sec followed by 50 cycles of two-step PCR, at 95°C for 3 sec and at
470 60°C for 30 sec with the fast 7500 mode; followed by 4) SNP assay (post-read) at 60°C for 30 sec
471 using ABI 7500 Fast Dx Real-Time PCR Instrument with SDS Software (ThermoFisher
472 Scientific). The genotype at each key position for each sample was determined by reading the
473 component signal of the amplification and the allelic discrimination analysis software in the
474 program.

475
476 **Whole genome sequencing.** Extended Data Fig. 2 displays a flowchart outlining samples available
477 for this study. Isolates with cycle threshold (Ct) values below 35 were selected for sequencing
478 using the ARTIC v3 low-cost protocol targeting 400bp amplicons³³ or Rapid Barcoding kit
479 protocol targeting 1,200bp amplicons³⁴. Briefly, RNA was extracted using the Qiagen RNeasy
480 Mini kit or Zymo DNA/RNA Mini kit. Reverse transcription was performed using LunaScript RT
481 SuperMix (NEB). Tiling PCR was performed on the cDNA, and amplicons were barcoded using
482 the Oxford Nanopore Native Barcoding Expansion 96 kit. Pooled barcoded libraries were then
483 sequenced on an Oxford Nanopore MinION sequencer using R9.4.1 flow cells. Basecalling was
484 performed in the MinKNOW software v21.02.1. Sequencing runs were monitored in real-time
485 using RAMPART (<https://artic-network.github.io/rampart/>) to ensure sufficient genomic coverage
486 with minimal runtime. Consensus sequence generation was performed using the ARTIC
487 bioinformatics pipeline (<https://github.com/artic-network/artic-ncov2019>). Genomes were

488 manually curated by visually inspecting sequencing alignment files for verification of key residues
489 in Geneious v10.2.6.

490

491 **Phylogenetic analysis.** Phylogenetic reconstruction of amino acid changes (Fig. 2A) was
492 conducted using the Nextstrain³⁵ workflow at <https://github.com/nextstrain/ncov> which aligns
493 sequences against the Wuhan-Hu-1 reference via nextalign
494 (<https://github.com/nextstrain/nextclade>), constructs a maximum-likelihood phylogenetic tree via
495 IQ-TREE³⁶, estimates molecular clock branch lengths via TreeTime³⁷ and reconstructs nucleotide
496 and amino acid changes also via TreeTime. This workflow was applied to 2309 SARS-CoV-2
497 genomes possessing the 9bp deletion Δ 106-108 in ORF1a-nsp6 along with mutation A20262G
498 which demarcates the parent clade to lineage B.1.526 alongside 688 global reference viruses. This
499 analysis was conducted on data downloaded from gisaid.org³⁸ on April 5, 2021. Phylogeographic
500 reconstruction of spread from New York state (Fig. 4E-F) was similarly conducted using the same
501 Nextstrain workflow with the addition of performing ancestral trait reconstruction of the
502 geographic “division” attribute of 933 SARS-CoV-2 genomes downloaded from gisaid.org on Jun
503 6, 2021.

504

505 **Neutralization studies of pseudoviruses.** We assayed the neutralizing activity of monoclonal
506 antibodies (mAbs), convalescent plasma, and vaccinee sera against E484K, S477N, and WT
507 (D614G) pseudoviruses, as well as pseudovirus NY Δ 5 containing all five signature mutations of
508 B.1.526-E484K (L5F, T95I, D253G, E484K, D614G, A701V), as previously described²⁷. We
509 examined four mAbs with emergency use authorization (CB6, REGN10987, REGN10933 and
510 LY-CoV555), plus eight additional RBD mAbs, including ones from our own collection (2-15, 2-
511 7, 1-57, & 2-36)²⁷ as well as S309³⁹, COV2-2196 & COV2-2130⁴⁰, and C121⁴¹. We also examined
512 convalescent plasma collected in Spring of 2020 (n=20 patients), and Moderna and Pfizer vaccinee
513 sera (n=22)⁴. Briefly, Vero E6 cells (ATCC) were seeded in 96-well plates (2×10^4 cells per well).
514 Pseudoviruses were incubated with serial dilutions of the test samples in triplicate for 30 min at
515 37 °C. The mixture was added to cultured cells and incubated for an additional 24 h. Luminescence
516 was measured using a Britelite plus Reporter Gene Assay System (PerkinElmer), and IC₅₀ was
517 defined as the dilution at which the relative light units were reduced by 50% compared with the
518 virus control wells (virus + cells) after subtraction of the background in the control groups with

519 cells only. The IC₅₀ values were calculated using nonlinear regression in GraphPad Prism 8.0.
520 Statistical analysis was performed using a Wilcoxon matched-pairs signed rank test. Two-tailed p-
521 values are reported.

522
523 **Neutralization of infectious SARS-CoV-2.** Infectious SARS-CoV-2 isolate hCoV-19/USA/NY-
524 NP-DOH1/2021 was isolated at the Aaron Diamond AIDS Center (Columbia University Medical
525 Ctr) from nasopharyngeal swab and propagated for one passage in Vero E6 cells (ATCC).
526 Infectious titer of the resulting virus was determined by an end-point dilution and cytopathic effect
527 (CPE) assay on Vero-E6 cells as described previously²⁷. The virus has since been deposited at BEI
528 Resources (Cat#NR-55359). SARS-CoV-2 virus USA-WA1/2020 (WA1) obtained from BEI
529 Resources (Cat# NR-52281) served as the control in experiments.

530
531 An end-point dilution microplate neutralization assay was performed to measure the neutralization
532 activity of twenty patient convalescent plasma samples and twelve purified monoclonal antibodies.
533 In brief, plasma samples were subjected to successive 5-fold dilutions starting from 1:100.
534 Similarly, antibodies were serially diluted (5-fold dilutions) starting at 50 µg/ml. Triplicates of
535 each dilution were incubated with SARS-CoV-2 at an MOI of 0.1 in EMEM with 7.5% inactivated
536 fetal calf serum (FCS) for 1 hour at 37°C. Post incubation, the virus-antibody mixture was
537 transferred onto a monolayer of Vero-E6 cells grown overnight. The cells were incubated with
538 the mixture for ~70 hours. Cytopathic effect (CPE) of viral infection was visually scored for each
539 well in a blinded fashion by two independent observers. The results were then converted into
540 percentage neutralization at a given sample dilution or antibody concentration, and the averages ±
541 SEM were plotted using a five-parameter dose-response curve in GraphPad Prism v8.4.

542
543 **Growth dynamics.** Growth dynamics of B.1.1.7 and B.1.526 were obtained through by
544 downloading “metadata” from gisaid.org on June 6, 2021 for all 422,760 viruses sampled from the
545 USA collected after January 1, 2021. This metadata has PANGO lineages⁴² already assigned to
546 each genome sequence. Daily state-level frequencies (and frequencies for CUIMC) were extracted
547 for plotting via 7-day sliding window averages of the prevalence of B.1.1.7 and B.1.526, calculated
548 as the number of sequence-verified samples from each strain divided by the total number of
549 positive samples with cycle threshold (Ct) values below 35, as this threshold value was used for

550 sequencing. Separately, a multinomial logistic regression model was fit directly to the observation
551 data consisting of individual genomes, their dates of sampling (independent variable X in days
552 since January 1, 2021) and their categorical labels (dependent variable Y , “B.1.1.7”, “B.1.526” and
553 “other”). This results in a 4-parameter model where both B.1.1.7 and B.1.526 have parameters
554 specified for frequency at day 0 (January 1, 2021) and logistic growth rate. This model was fit to
555 the data using the Classify package of Mathematica v12.2.

556
557 **Data availability.** All genomes and associated metadata generated as a part of this study have been
558 uploaded to GISAID. Biological materials (i.e. variant pseudoviruses) generated as a part of this
559 study will be made available but may require execution of a materials transfer agreement.

560
561 **Code availability.** Data processing and visualization was performed using publicly available
562 software and packages, primarily RStudio v1.2.5033, GraphPad Prism v8.4, and iTOL
563 (<https://itol.embl.de/>). The exact workflow used for phylogenetic (Fig. 2A) and phylogeographic
564 analysis of public GISAID data (Fig. 4E-F) is available at <https://github.com/blab/ncov-ny>.
565 Frequency dynamics were modeled using Mathematica in notebooks also available at
566 <https://github.com/blab/ncov-ny>.

567
568 **Methods References**

- 569 32 Smyrlaki, I. et al. Massive and rapid COVID-19 testing is feasible by extraction-free
570 SARS-CoV-2 RT-PCR. Nat Commun 11, 4812, doi:10.1038/s41467-020-18611-5 (2020).
- 571 33 Quick, J. Artic Protocol, <[https://www.protocols.io/view/ncov-2019-sequencing-protocol-
572 v3-locost-bh42j8ye](https://www.protocols.io/view/ncov-2019-sequencing-protocol-v3-locost-bh42j8ye)> (2021).
- 573 34 Freed, N., Vlkova, M., Faisal, M. B. & Silander, O. Rapid and inexpensive whole-genome
574 sequencing of SARS-CoV2 using 1200 bp tiled amplicons and Oxford Nanopore rapid
575 barcoding. bioRxiv, doi:10.1101/2020.05.28.122648 (2020).
- 576 35 Hadfield, J. et al. Nextstrain: real-time tracking of pathogen evolution. Bioinformatics 34,
577 4121-4123, doi:10.1093/bioinformatics/bty407 (2018).
- 578 36 Minh, B. Q. et al. IQ-TREE 2: New Models and Efficient Methods for Phylogenetic
579 Inference in the Genomic Era. Mol Biol Evol 37, 1530-1534, doi:10.1093/molbev/msaa015
580 (2020).

- 581 37 Sagulenko, P., Puller, V. & Neher, R. A. TreeTime: Maximum-likelihood phylodynamic
582 analysis. *Virus Evol* 4, vex042, doi:10.1093/ve/vex042 (2018).
- 583 38 Shu, Y. & McCauley, J. GISAID: Global initiative on sharing all influenza data - from
584 vision to reality. *Euro Surveill* 22, doi:10.2807/1560-7917.ES.2017.22.13.30494 (2017).
- 585 39 Pinto, D. et al. Cross-neutralization of SARS-CoV-2 by a human monoclonal SARS-CoV
586 antibody. *Nature* 583, 290-295, doi:10.1038/s41586-020-2349-y (2020).
- 587 40 Zost, S. J. et al. Rapid isolation and profiling of a diverse panel of human monoclonal
588 antibodies targeting the SARS-CoV-2 spike protein. *Nat Med* 26, 1422-1427,
589 doi:10.1038/s41591-020-0998-x (2020).
- 590 41 Robbiani, D. F. et al. Convergent antibody responses to SARS-CoV-2 in convalescent
591 individuals. *Nature* 584, 437-442, doi:10.1038/s41586-020-2456-9 (2020).
- 592 42 Rambaut, A. et al. A dynamic nomenclature proposal for SARS-CoV-2 lineages to assist
593 genomic epidemiology. *Nat Microbiol* 5, 1403-1407, doi:10.1038/s41564-020-0770-5
594 (2020).

595

596

597 **Acknowledgements:** Biospecimens utilized for this research were obtained from the Columbia
598 University Biobank (CUB) with technical support from Viplan J. Mahadeva, Sebastian
599 Fernando and Sylvia T. Parker-Jones. CUB is supported by the Irving Institute for Clinical and
600 Translational Research (NCATS UL1TR001873). In particular, we thank Muredach Reilly, Eldad
601 Hod, and the CUB COVID-19 Genomics Consortium (CCGC) for facilitating this effort. We are
602 also grateful to Lihong Liu and Sho Iketani for technical support, and Alan Perelson for
603 mathematical input. We gratefully acknowledge all the authors, the originating laboratories
604 responsible for obtaining the specimens, and the submitting laboratories for generating the genetic
605 sequence and metadata and sharing via the GISAID Initiative, on which part of the presented
606 research is based (see Supplementary Table 1). This work was in part funded by NIH/NIDA grant
607 U01 DA053949 (A.-C.U, M.K.A.) and by support from Andrew & Peggy Cherng, Samuel Yin,
608 Barbara Picower and the JBP Foundation, Bria Biosciences, Roger & David Wu, and the Bill and
609 Melinda Gates Foundation. T.B. is a Pew Biomedical Scholar and is supported by NIH grant no.
610 R35 GM119774-01. Funders and funding agencies had no role in study design, data collection and
611 analysis, decision to publish, or preparation of the manuscript.

612

613 **Competing Interests:** P.W., M.S.N., Y.H., and D.D.H. are inventors on a provisional patent
614 application on monoclonal antibodies against SARS-CoV-2. D.D.H. is a member of the scientific
615 advisory board of Bii Biosciences, which has provided a grant to Columbia University to support
616 this and other studies on SARS-CoV-2. A.-C.U. and D.D.H. have received funding from Merck &
617 Co. unrelated to this study.

618

619 **Author Contributions: Conceptualization** – A.-C.U., D.D.H., M.K.A., H.M.; **Data curation** –
620 M.K.A., H.M., J.E.Z., P.W., M.S.N., Z.S., T.B., A.G.-S., Y.H., A.L.K., M.T., A.-C.U.; **Formal**
621 **analysis** – M.K.A., P.W., J.E.Z., T.B., A.G.-S.; **Funding acquisition** – A.-C.U., D.D.H., M.K.A.;
622 **Investigation** – M.K.A., H.M., J.E.Z., P.W., M.S.N., A.L.K., M.T., T.B., Y.H.; **Methodology** –
623 M.K.A., H.M., P.W., M.S.N., T.B., Y.H.; **Supervision** – A.-C.U., D.D.H.; **Visualization** –
624 M.K.A., P.W., T.B.; **Writing – original draft** – A.-C.U., M.K.A., H.M., D.D.H.; **Writing –**
625 **review and editing** – all authors

626

627 Supplementary Information is available for this paper.

628

629 Correspondence and requests for materials should be addressed to Anne-Catrin Uhlemann
630 (au2110@cumc.columbia.edu) or David D. Ho (dh2994@cumc.columbia.edu).

631

632 **Extended Data**

Extended Data Table 1. Clinical characteristics of patients infected with SARS-CoV-2 based on viral genotype

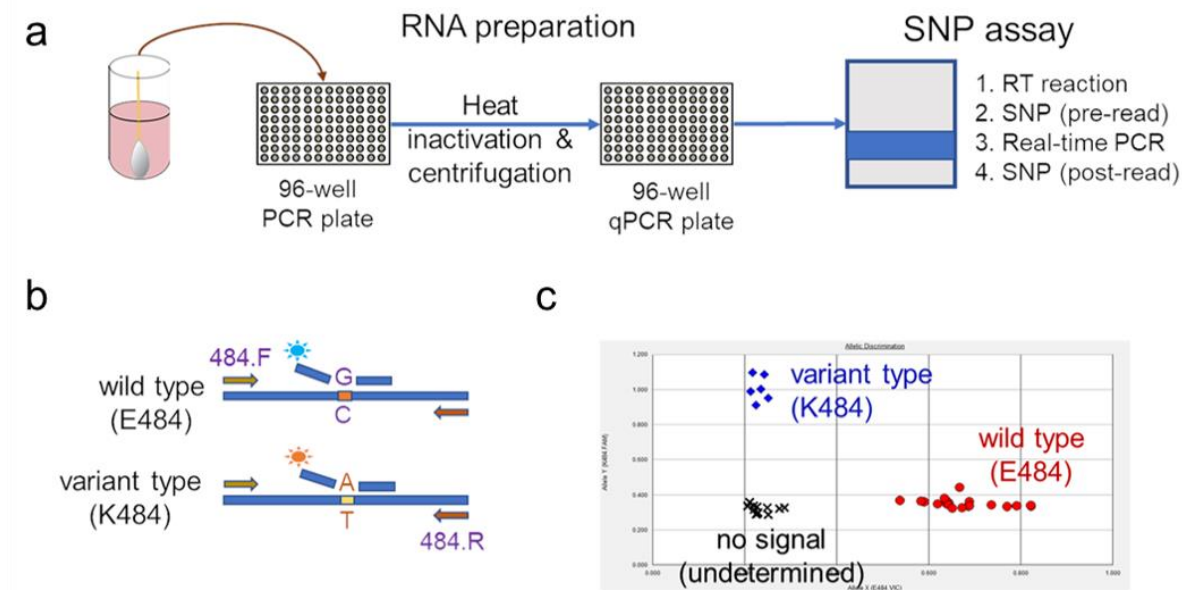
Clinical Characteristic	E484K (n=148)	Wildtype ¹ (n=1,124)	P ²	Non-VOI/VOC lineages ¹		P ²
				B.1.526-E484K (n=192)	(n=660)	
Demographics						
Male sex, n (%)	71 (48.0)	507 (45.1)	0.575	81 (42.2)	316 (48.0)	0.179
Age, years (median [IQR])	58 [38, 71]	55 [32, 71]	0.354 ³	49 [32, 71]	52 [30, 68]	0.778 ³
Race and ethnicity, n (%)			0.524			0.562
Hispanic/Latino	74 (50.0)	520 (46.3)		99 (51.6)	304 (46.2)	
Black	11 (7.4)	122 (10.9)		21 (10.9)	74 (11.2)	
White	19 (12.8)	164 (14.6)		21 (10.9)	90 (13.7)	
Other	44 (29.7)	317 (28.2)		51 (26.6)	190 (28.9)	
Place of residence, n (%)			0.017			0.011
NYC	129 (87.2)	909 (80.9)		166 (86.5)	521 (78.9)	
Yonkers	7 (4.7)	31 (2.8)		8 (4.2)	19 (2.9)	
Outside NYC and Yonkers	12 (8.1)	184 (16.4)		18 (9.4)	120 (18.2)	
Comorbidities						
BMI, kg/m ² (median [IQR])	28.6 [24.9, 33.5]	27.3 [23.4, 31.4]	0.064 ³	28.4 [24.3, 33.1]	26.5 [23.0, 30.1]	0.008 ³
Hypertension, n (%)	66 (45.2)	424 (41.4)	0.435	73 (39.5)	243 (40.5)	0.868
Diabetes mellitus, n (%)	47 (32.2)	247 (24.1)	0.045	57 (30.8)	130 (21.7)	0.014
Chronic kidney disease, n (%)	19 (13.0)	113 (11.0)	0.571	15 (8.1)	79 (13.2)	0.085
Coronary artery disease, n (%)	12 (8.2)	97 (9.5)	0.737	13 (7.0)	52 (8.7)	0.579
Solid organ transplant, n (%)	4 (2.7)	38 (3.7)	0.725	7 (3.8)	35 (5.8)	0.370
Cycle threshold value (mean (SD))⁴	29.49 (5.57)	30.71 (5.64)	0.013	27.33 (4.57)	28.31 (4.74)	0.041
Severity of care and outcomes						
Highest level of care, n (%)			0.281			0.041
Admitted	48 (32.4)	393 (35.1)		69 (35.9)	185 (28.2)	
Emergency Department	55 (37.2)	321 (28.6)		65 (33.9)	201 (30.6)	
ICU	11 (7.4)	86 (7.7)		12 (6.2)	52 (7.9)	
Outpatient	34 (23.0)	320 (28.5)		46 (24.0)	219 (33.3)	
Supplemental oxygen, n (%)	46 (86.8)	327 (76.2)	0.118	55 (79.7)	155 (71.4)	0.230
Outcome, n (%)			0.293			0.482
Deceased or discharged to hospice	7 (4.7)	86 (7.7)		8 (4.2)	37 (5.6)	
Further care at external facility	15 (10.1)	76 (6.8)		15 (7.9)	38 (5.8)	
Discharged to home	126 (85.1)	956 (85.4)		167 (87.4)	579 (88.4)	

¹ Wildtype isolates are defined as those without E484K or N501Y mutations. For comparisons based on lineage, B.1.526-E484K was compared with non-variant of interest (VOI) and non-variant of concern (VOC) lineages (i.e. B.1.526.1, B.1.526.2, B.1.1.7, P.1, P.2, and B.1.351 were excluded)

² T-tests were performed for continuous variables and chi-squared tests for categorical variables, unless otherwise indicated as below

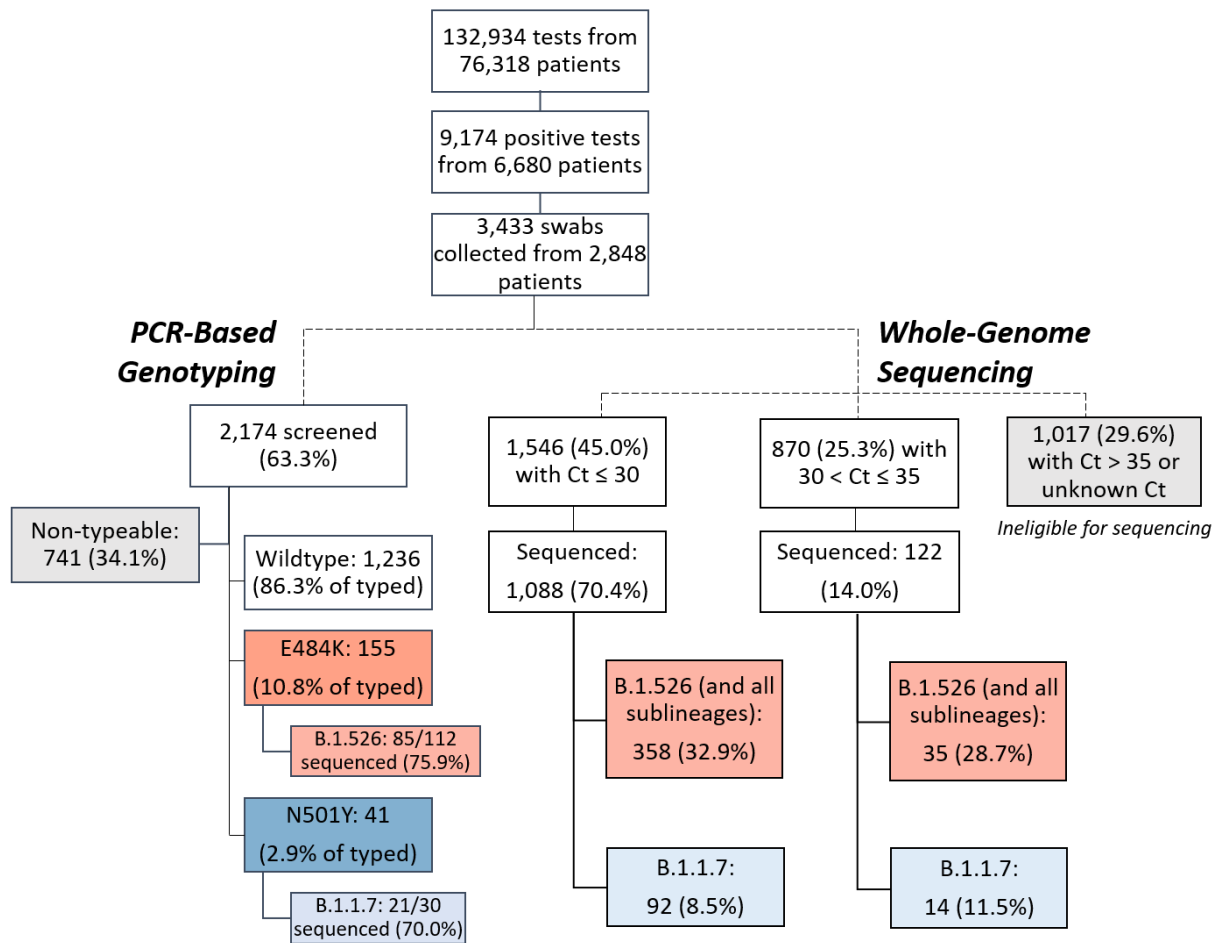
³ Due to non-normal distribution, Kruskal-Wallis non-parametric test was used

⁴ Cycle threshold value as determined through our rapid qPCR-based screening assay on heat-inactivated nasopharyngeal swab samples



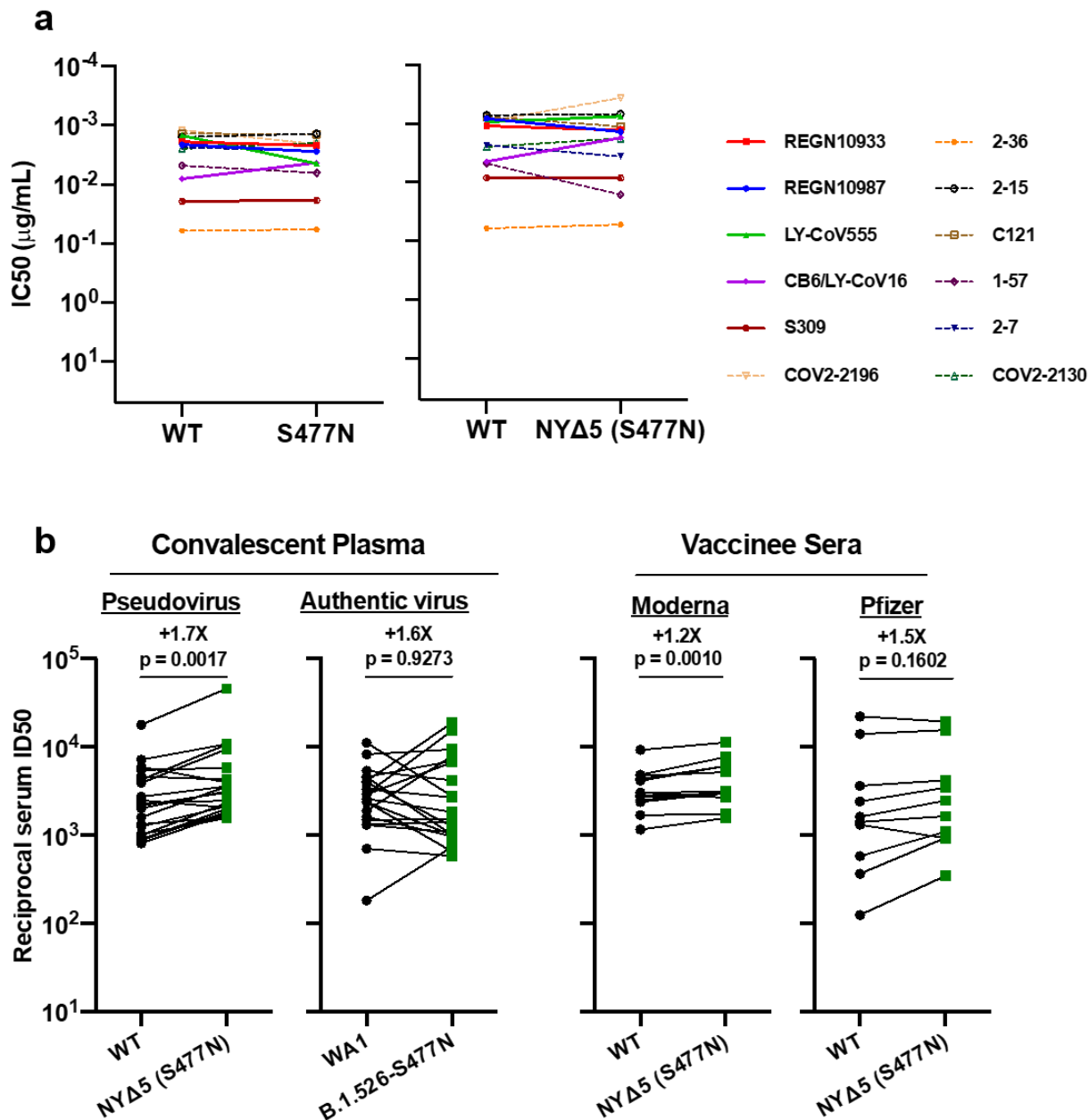
Extended Data Figure 1. Rapid PCR-based screening assay protocol to identify samples harboring key substitutions. (a) Viral RNA is prepared by heat inactivation and centrifugation. The supernatant is then used for the SNP assay, which entails four steps: the reverse transcription (RT) reaction, pre-PCR reading of the plate to assess background fluorescence (SNP pre-read), real-time PCR, and post-PCR reading of the plate to measure fluorescence (SNP post-read). The runtime for this entire protocol is approximately two hours. (b) Genotype at targeted sites in COVID-19 viral RNA can be determined with two MGB probes, one for wild type (conjugated with VIC) and the other for variant type (conjugated with FAM). (c) Example signals for the variant type (K484; blue), the wild type (E484; red) and samples with no signal (black) are shown.

633

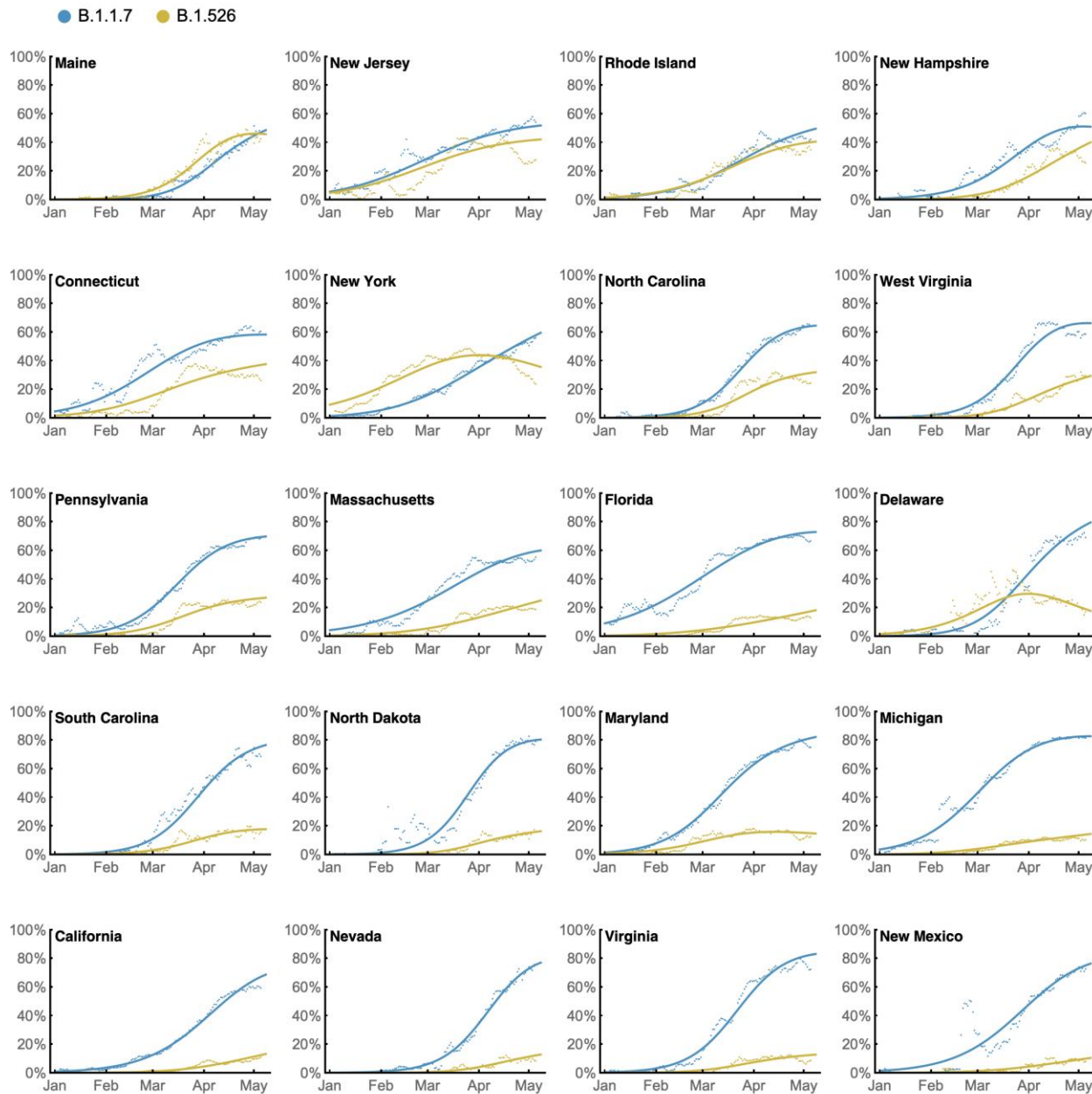


Note: 1 swab identified with E484K and N501Y was sequence-verified as B.1.351

Extended Data Figure 2. Flowchart for SARS-CoV-2-positive nasopharyngeal swabs included in this study. (top) During the study period of November 1, 2020 to May 1, 2021, 6,680 patients tested positive for SARS-CoV-2 at our hospital center and affiliated hospitals. From these 9,174 positive nasopharyngeal swabs, 3,433 swabs were stored as part of the Columbia University Biobank effort to archive samples during the COVID-19 pandemic. (left) PCR-based genotyping assays for E484K and N501Y (see Extended Data Fig. 1) were performed on 2,174 samples collected in the early phase of this study, between November 1, 2020 and March 1, 2021. We identified a significant proportion of samples with E484K (10.8%), later confirmed through sequencing to primarily fall within the B.1.526 lineage, and a number of samples with N501Y (2.9%), primarily within the B.1.1.7 lineage. (right) We performed whole-genome sequencing on 1,210 samples during the full study period, until May 1, 2020. Of these, 32.5% belonged to B.1.526 and the sublineages B.1.526.1 and B.1.526.2, while B.1.1.7 constituted a much smaller proportion of samples at our center (8.8%).



Extended Data Figure 3. Neutralization studies of B.1.526-S477N. (a) Neutralizing activities of 12 monoclonal antibodies against pseudoviruses containing S477N alone or all five signature B.1.526-S477N mutations (L5F, T95I, D253G, A701V, and S477N), termed NY Δ 5(S477N). Antibodies with emergency use authorization are shown in bold solid lines. (b) Neutralizing activities of convalescent plasma (n=20) against NY Δ 5(S477N) as well as against the authentic B.1.526 virus with S477N, and neutralizing activities of vaccinee sera (n=22) against the NY Δ 5(S477N) pseudovirus, compared to wildtype counterparts.



636
637

638 **Extended Data Figure 4. State-level growth dynamics of B.1.526 and B.1.1.7.** Daily state-level
639 frequencies of B.1.526 (in yellow) and B.1.1.7 (in blue), based on GISAID data downloaded on
640 June 6, 2021, were used to plot 7-day sliding window averages of the prevalence of each lineage
641 (shown as dots in the figure). A 4-parameter multinomial logistic regression model was fit directly
642 to the observation data, in which both B.1.1.7 and B.1.526 have parameters specified for frequency
643 at day 0 (January 1, 2021) and logistic growth rate (shown as lines in the figure). States are ordered
644 according to frequency of B.1.526 at the final timepoint of May 8, 2021.